CANARY Phase B: the LGS upgrade to the CANARY tomographic MOAO pathfinder

T. Morris[1a], Z. Hubert[2], F. Chemla[3], S. Todd[4], E. Gendron[2], J-M. Huet[3], E. Younger[1], A. Basden[1], N. Dipper[1], D. Geng[1], D. Atkinson[4], M. Marteaud[2], A. Longmore[4], P. Clark[1], D. Henry[4], C. Dickson[4], F. Vidal[2], M. Black[4], P. Laporte[3], C. Dunlop[1], J. Skvarc[5], D. Cano[5], G. Talbot[1], G. Rousset[2], and R. Myers[1]

[1] University of Durham, Department of Physics, South Road, Durham, DH1 3LE, UK
[2] LESIA, Observatoire de Paris, 5, Place Jules Janssen, 92195 Meudon Cedex, France
[3] GEPI, Observatoire de Paris, 5, Place Jules Janssen, 92195 Meudon Cedex, France
[4] UK Astronomy Technology Centre, Royal Observatory, Edinburgh, Blackford Hill, Edinburgh, EH9 3HJ, UK
[5] Isaac Newton Group of Telescopes, Edificio Mayantigo, Calle Alvarez Abreu, 70, E-38700 Santa Cruz de la Palma, Canary Islands, Spain

Abstract. CANARY has been designed to demonstrate full tomographic LGS MOAO in a configuration as close as possible to that of the proposed EAGLE instrument for the E-ELT. A phased approach to the instrument development has been adopted to reduce the overall risk and developmental complexity with the initial Phase A system performing NGS MOAO only using three off-axis NGS WFS. The Phase B system will add four off-axis open-loop LGS WFSs to this system allowing combined LGS/NGS tomography to be performed, thereby taking CANARY one step closer to an EAGLE-like configuration. The upgrade to include LGS within CANARY requires several new and upgrades subsystems, including a multiple LGS launch system, LGS WFSs and a new LGS calibration unit. Here we present the requirements, design, and subsystem performance for the Phase B system, as well as simulations of the on-sky AO performance of CANARY Phase B.

1 Introduction

CANARY is an open-loop tomographic adaptive optics (AO) demonstrator that was designed for use at the 4.2m William Herschel Telescope (WHT) in La Palma. Due to the complexity of this system a phased approach to system development was adopted. Phase A implemented Natural Guide Star (NGS) based tomographic correction [1] using three off-axis NGS Wavefront Sensors (WFS). The Phase A system was commissioned on sky in September 2010 where it performed the first demonstration of open-loop adaptive optics correction using off-axis natural guide stars [2,3]. Phase B of the project extends the original system functionality to also include the ability to measure wavefronts from four off-axis Rayleigh laser guide stars. This paper first gives an overview of the upgrades that will be made to the Phase A system to allow it to perform Laser Guide Star (LGS) tomography and then presents initial error budget and analysis for the Phase B system.

2 Phase B upgrade overview

The upgrade path to allow CANARY to perform LGS WFSing was included within the design from the outset of the project. The initial CANARY design concept described a modular system that would minimise the effort associated with system reconfiguration between the various phases of CANARY. The addition of LGS WFSing functionality to the system entails a minor reconfiguration of the original Phase A system and integrating several new opto-mechanical and software modules.

Here we describe the design and performance of the major Phase B subsystems and the upgrade to the instrument control systems. It should be noted that in the light of on-sky experience from Phase

[a] t.j.morris@durham.ac.uk

A there have also been several small changes to various Phase A subsystems to improve the overall system ease of use which have not been described here.

2.1 Telescope simulator

The telescope simulator is the principal means of both system alignment and off-sky performance characterisation. At Phase B, the Telescope Simulator is being upgraded to include new LGS reference sources and a wedge plate that will allow the measurement of LGS WFS to deformable mirror (DM) interaction matrices. The telescope simulator must be able to reproduce any LGS asterism that could be observed with CANARY, meaning that the asterism spacing and conjugate altitude must be adjustable.

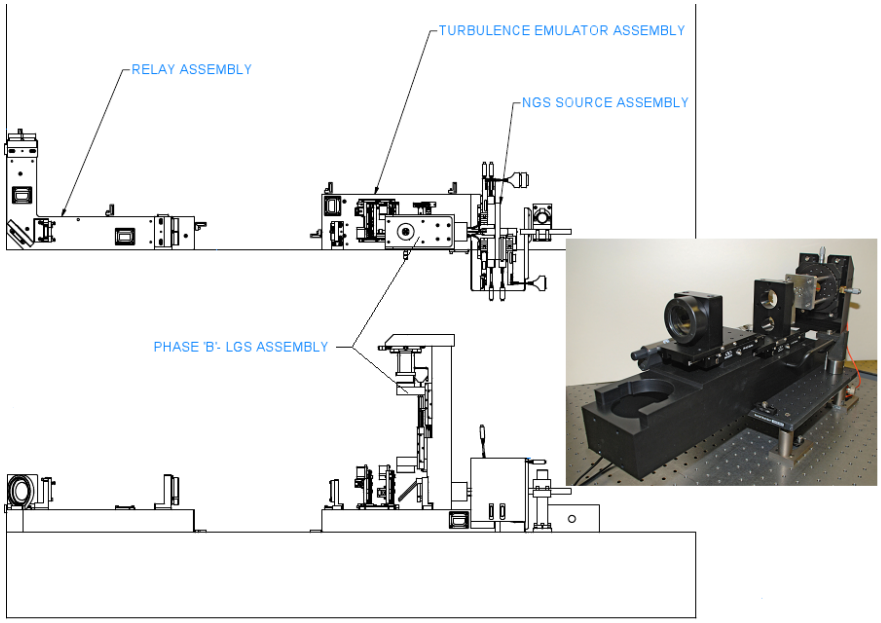

Fig. 1. Phase B telescope simulator layout on optical bench. Image shows assembled LGS arm in horizontal test configuration during AIT

The LGS WFS reference sources are fibre-coupled green light emitting diodes (LEDs) that are placed in a separate LGS arm that is coupled into the optical train using a plate beam-splitter. The LGS source altitude can be changed over a range of 11-21km, and the asterism diameter changed by replacing the machined plate in which the sources are held.

One of the procedures of the system calibration at Phase A compared the influence functions and alignment of the DM actuators as observed the open-loop NGS WFSs that observed by the closed-loop Truth Sensor. To achieve this, a reverse path calibration source was included within the system. This source illuminated the AO path in reverse and fed light (via retro-reflection in front of the focal plane) to the NGS WFSs in turn. This approach cannot be used at Phase B because the tilted dichroic means the LGS WFSs cannot observe the DM directly. A wedged plate will therefore be placed at a pupil plane within the telescope simulator. When this plate is rotated, all NGS and LGS WFSs in the system will observe the same angular tip and tilt. By comparing the WFS spot motion for identical subapertures on different WFSs the link between LGS WFS spot motion and DM influence functions can be established.

2.2 Laser launch system

The existing WHT laser launch system will be modified to create a 4 Rayleigh LGS asterism within the CANARY field of view of 2.5'. The LGS asterism will be of a radius and at an altitude that provides optimal AO correction along a single line of sight for a defined set of atmospheric parameters. The asterism must remain fixed with respect to the background NGS.

Upgrades to the existing WHT laser launch system [5] will be installed at the beginning of October 2011. Two pulsed 16W 532nm lasers are combined both spatially and temporally and then sent through the existing WHT beam launch optics to create the Phase B LGS. An etched-glass diffractive optical element (DOE) is used to split the combined beam into the 4 beams required for the Phase B asterism. The DOE is placed within a rotation stage so that the LGS asterism remains fixed on-sky. This approach is similar to that used at the MMT laser launch system [4].

The co-alignment of the two lasers is actively controlled via two steering mirrors at the output of one of the lasers. Temporal synchronisation of the output laser pulses is monitored via a high-speed photodiode and controlled by offsetting trigger pulses to the lasers. Synchronisation of the laser pulses is limited by jitter to less than 30ns, equating to a wavefront error due to laser focus of 58nm P-V, or approximately 19nm RMS at the nominal LGS altitude of 15km. This error term increases to 44nm RMS at the lowest observable range gate distance of 10km.

CANARY is a single channel MOAO (multiple object AO) system therefore the performance can be optimised for the on-axis direction only allowing use of the optimal LTAO (laser tomographic AO) asterism. The optimum asterism diameter has been theoretically calculated to be between 0.85 and 0.95 of the pupil diameter for any given LGS focal distance above the telescope (see Fig. 2).

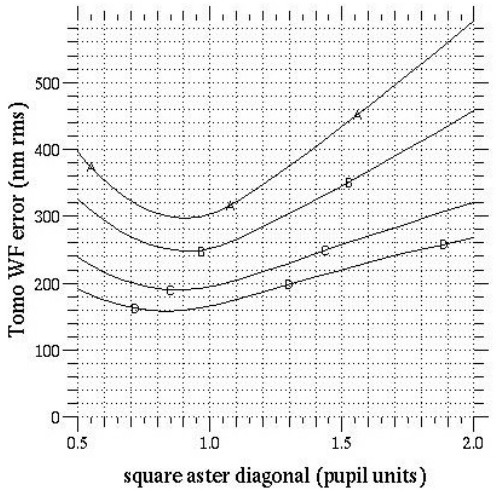

Fig. 2. RMS wavefront error due to tomographic reconstruction for LGS of various altitudes as a function of LGS asterism diameter (expressed as the number of pupils diameters across the diagonal of the asterism). Lines A-D represent LGS altitudes at 8, 10, 15 and 20km respectively.

The beam combiner efficiency has been measured and the combined beam outputs 30W. The 2-layer DOE places a measured 64% of the light into the 1st diffracted order. With this efficiency, a 400m LGS at 15km should provide 450 photons/subaperture/frame at 300Hz. This value includes a significant flux margin that will allow the system to cope with varying atmospheric conditions. The 15km distant, 400m deep LGS has been defined as the baseline LGS throughout the Phase B design process, but higher altitude guide stars provide better tomographic performance. The true optimal LGS altitude and asterism diameter is dependent upon atmospheric turbulence profile and atmospheric transmission.

2.3 LGS wavefront sensor

The LGS WFS will observe the four off-axis LGS created by the laser launch system. All the LGS are imaged using a single detector with an integrated electronic shutter that allows us to temporally range gate the Rayleigh backscattered photon return from the laser pulses. The shutter has a measured contrast ratio of over 1000:1 at the laser wavelength. A 7x7 subaperture Shack-Hartmann pattern from each LGS is imaged onto a 64x64 pixel quadrant of the detector, providing 8x8 pixels per subaperture. Each subaperture has a field of view of 4.8".

The flexibility of investigating alternative LGS asterism diameters and altitudes is key to characterising and understanding the tomographic performance of the LGS system. This is particularly important on a 4.2m diameter telescope such as the WHT where the Rayleigh LGS pupils separate at a low altitude, thereby limiting the tomography to 3-4km above the telescope.

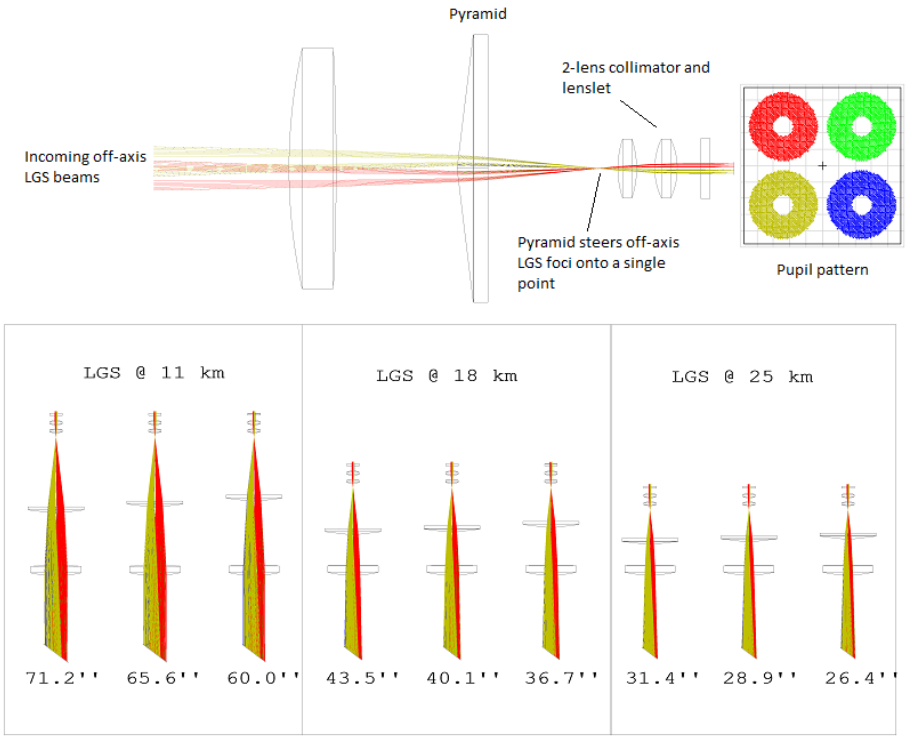

Fig. 3. LGS WFS pyramid field selector. Upper: Optical layout for the pyramid LGS field selector showing collimated LGS beams after tip-tilt correction, passing through the focusing lens and into the pyramid. The pyramid is positioned such that the off-axis LGS are refracted towards a single 4-5" field stop conjugated to the focal distance defined by the LGS range-gate. The lens spacing in a 2-lens system is precisely tuned to collimate the four off-axis beams and re-image the four pupil images onto a single 17×17 lenslet array. The four resultant 7×7 spot patterns are then re-imaged onto the LGS WFS detector. Lower: The pyramid and post-pyramid optics location for 9 different LGS asterisms. The diagonal diameter across the square asterism is given in arcseconds below each optical layout.

To fit the four LGS WFS patterns on to a single detector and allow observation of a wide range of LGS asterisms, a simple 2 element system is used to select both the altitude and off-axis angle of the LGS. The selection of the asterism is achieved by a novel field selector that utilises a pyramidal prism. By adjusting the distance between the LGS focal plane, the pyramid and subsequent LGS WFS optics,

a range of square asterisms can be observed between 11 and 25km (see Fig. 3). Asterism radii around the optimal values of 0.8-1 × pupil diameter can be observed over this range of LGS focal distances. There is a lower limit to the asterism diameter that occurs when beams overlap at the pyramid vertices. The technique of using a pyramid to select the asterism diameter and altitude would be suitable for any rotationally symmetrical guide star pattern, even if multiple WFS detectors were available.

Transmission of the LGS light through the pyramidal prism does introduce wavefront aberrations however these are static for a given asterism and can be removed using calibration sources positioned at a prior LGS focal plane. In CANARY, the magnitude of the expected aberration will not offset the centroid within any given sub-aperture by more than 0.3", leaving (at least) a 4.5" field of view to contain the elongated LGS Shack-Hartmann (SH) pattern.

The LGS WFS path also contains a tip-tilt mirror for the correction of LGS launch jitter capable of ±4" of on-sky motion at bandwidths of up to 150Hz. This tip-tilt mirror is common to each of the LGS, so can only remove tip-tilt motion caused by telescope vibration and ground layer turbulence. Monte-Carlo simulations [6] of the correction of the atmospheric contribution to this term show that we can expect to see a $\pm 1\sigma$ spot motion after correction of 0.3" for the standard CANARY atmosphere.

Due to poor weather the number of on-sky nights at Phase A was limited. The decision was made to fit the LGS WFS around the existing layout to revert to the original Phase A system for gathering additional data if required. Although the inclusion of an LGS pickoff path was always envisaged within the system design, the requirement that we must be able to revert to a Phase A configuration was not. The only feasible option was to place a dichroic in front of the input NGS focal plane and direct the LGS wavelengths to a second bench placed above the main AO path. The LGS light is picked off by a 532nm Rugate notch filter before the NGS focal plane and the light directed upwards through the existing NGS WFS support structure. By removing the LGS dichroic, the system is returned to the same configuration as it was at Phase A.

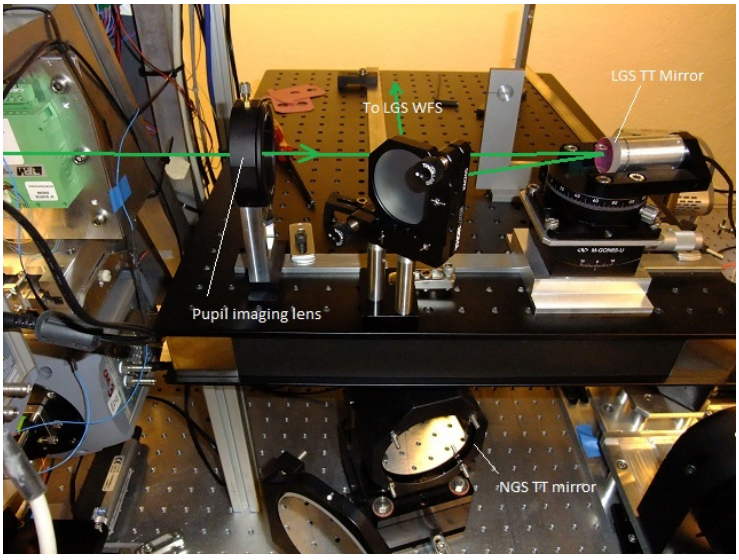

Fig. 4. LGS WGS upper bench, pupil re-imaging system and LGS tip-tilt mirror installed above main AO path during AIT.

Passage through the tilted LGS dichroic introduces aberrations into the transmitted NGS/science light paths. Defocus can be removed by the telescope, but approximately 400nm RMS residual wavefront error will be observed after the 6mm thick dichroic. This aberration can be corrected by the deformable mirror by using approximately 9% of its available stroke. The residual error after DM correction will be less than 60nm RMS, but we are investigating including an astigmatic correction

element in front of the science camera to reduce this error further and limit the amount of stroke used by the DM in its correction. Aberrations due to the dichroic will be observed by all the open-loop NGS WFSs in the system but can be removed through the calibration process.

2.4 Instrument control

Whilst CANARY does contain modular interfaces for both instrument control and data transfer, it proved difficult to meet the requirement to provide contiguous wavefront data without missing frames using this interface. Network congestion, packet loss and data distribution overheads meant that a non-realtime direct socket interface was implemented to capture datasets from the real time control system (RTCS). This base architecture will remain unchanged for Phase B, but additional data streams will be captured to control LGS asterism pointing and rotation. A process has been developed to allow static offsets that build up on the LGS tip-tilt mirror to be offloaded to a steering lens in the laser launch system after any rotational misalignment of the 4 LGS SH patterns has been removed. This latter task is achieved via rotation of the launch system DOE.

Inside the laser launch system, a separate instance of the CANARY RTCS has been interfaced to the beam monitoring camera and controls the steering mirrors within the beam combiner system. This allows simple control of the beam combiner using the same interfaces developed for the main CANARY system. A remote interface for laser control has also been developed, although laser pulse synchronisation is not yet automated.

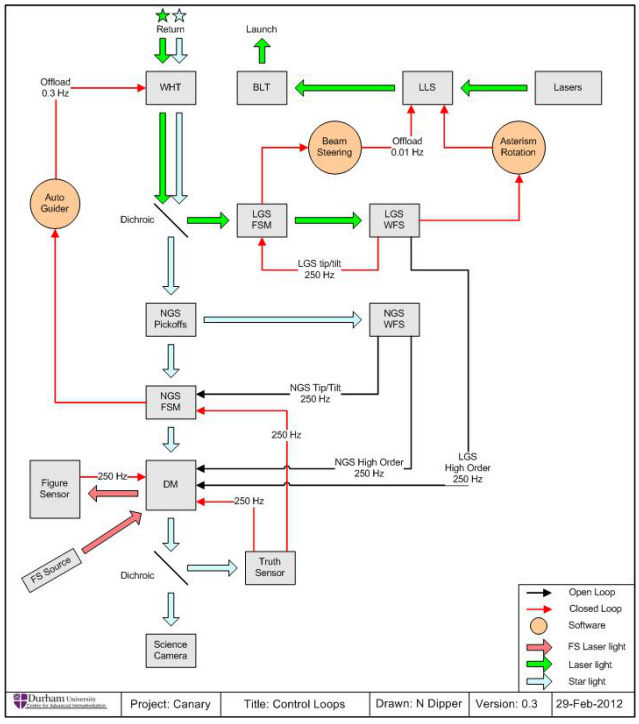

Fig. 5. LGS and NGS control loops and light path within the Phase B system. A default update rate of 250Hz has been indicated. Actual update rates range between 100 and 300Hz and is limited by the WFS readout speed. The beam combining control loop with the laser launch system is not shown.

3 Performance

In addition to the tomographic and closed-loop modes available at Phase A, Phase B will also be able to perform open-loop MOAO/LTAO and open-loop LGS GLAO (Ground Layer AO), with either single or multiple tip/tilt/focus NGS reference stars. CANARY is also capable of using all open-loop NGS and LGS WFSs simultaneously through modification of the control matrices within the RTCS. We are also implementing LQG control [7] within the real time control system in addition to the Learn and Apply [8] tomographic calibration used during Phase A. Here we describe the performance of only the standard operating modes of high-order (HO) LGS correction with a single on-axis tip-tilt (TT) reference star, and that achieved when performing tomography using HO wavefronts from all 4 LGS and 3 NGS WFSs.

The error budget presented here combines the results of Monte-Carlo simulations performed using the YAO platform[9] with additional error terms that could not be easily included within the simulation. These latter error terms were either measured during Phase A or calculated during the Phase B design process. Error terms that will be corrected before on-sky commissioning, such as those due to passage through the tilted dichroic (see Sect. 2.3), have not been included within the error budget presented in Table 1. Tomographic calibration has been performed using the Learn and Apply method.

Table 1. Phase B error budget showing contributions to the overall system performance. Error terms are separated into those simulated, those calculated and those unchanged and measured from the Phase A system. Strehl ratios have been calculated in the H-band at 1650nm

Error term	**Value (nm RMS)**	**Comment**
Monte-Carlo configuration:		
4 HO LGS + on-axis TT NGS	277	Strehl ratio of 33%
4 HO LGS + 3 off-axis HO NGS	300	Strehl ratio of 27%
Errors measured at Phase A:		
Static bench errors	160	Uncorrectable with existing DM
Calculated errors:		
DM open-loop error	48	
TT open-loop error	26	
LGS pulse synchronisation	19	Calculated for a 15km LGS
Total (on-axis TT NGS)	**325**	Strehl ratio of 22%
Total (3 $\times$ off-axis HO NGS)	**344**	Strehl ratio of 18%

Breaking down the simulated performance further, the principal terms in the Phase B error budget are tomographic error and the DM fitting error. Tomographic error is highly dependent on the vertical distribution of turbulence, so these results are only valid for the defined CANARY median atmosphere and must be recalculated for the actual turbulence profile encountered. Most of the measured/calculated terms in the error budget remain unchanged from the Phase A system, where the static bench error dominates. This error was principally caused by uncorrectable high spatial frequency polishing errors on the DM.

An accurate match between theory and practice is one of the main aims of the CANARY project, and the error budget presented here indicates a level of performance that is in the range where the on-sky results can be easily compared to those obtained from theory and simulations.

Although the level of correction that CANARY will be modest due to the low-order nature of the system, it should be noted that major Phase A/B error terms (fitting, tomographic and static high-frequency) will all be reduced with the inclusion of a higher-order DM and associated WFSs within the system which is planned for Phase C of CANARY.

4 Conclusion

We have presented the requirements and design overview of the new subsystems and software that form Phase B of CANARY. These subsystems will allow CANARY to perform open loop tomographic wavefront correction using up to 4 off-axis LGS in addition to the 3 off-axis NGS used at Phase A.

Monte-Carlo simulations of system performance have been completed and additional error terms not included within the simulation have been added to estimate the on-sky levels of correction that will be observed, showing open-loop H-band Strehl ratios in the range of 18-22% for typical conditions at the WHT.

CANARY is currently installed at the Observatoire de Paris in its phase A configuration. Phase B hardware integration begins at the end of October 2011. The RTCS has been interfaced to the Phase B hardware and tested, and the user interface software has been upgraded to handle LGS calibration and streamline the data acquisition process.

The Laser Launch system is currently in transit to the WHT and will undergo initial commissioning over two nights in November, with backup runs in March and April. Telescope time for phase B on-sky commissioning has been awarded at the end of July 2012.

References

1. T. Morris, Z. Hubert, R.Myers *et al.*, *1st AO4ELT Conference*, (2010) p08003
2. E. Gendron, F. Vidal, M. Brangier *et al.*, A&A **529**, (2011) pL2
3. E. Gendron, T. Morris, F. Vidal *et al.*, *this conference*, (2011)
4. J. A. Georges, P. Mallik, T. Stalcup *et al.*, Proc. SPIE **4839**, (2002) pp. 473-483
5. G. Talbot, D. Carlos Abrams, N. Apostolakos *et al.*, Proc SPIE **6272**, (2006) p62722H
6. A. Basden, T. Butterley, R. Myers and R. Wilson, Appl. Opt. **46**, (2007) pp. 1089-1098
7. C. Petit, J-M. Conan, C. Kulcsar and H-F. Reynaud, J. Opt, Soc. Am. A **26**, (2009) pp. 1307-1325
8. F. Vidal, E. Gendron and G. Rousset, J. Opt, Soc. Am. A **27**, (2010) pp. A253-A264
9. F. Rigaut, https://github.com/frigaut/yao